Supplementary Data

Atmospheric data can be accessed at:
atmos.washington.edu/jaffegroup/modules/archive/

Microarray data can be accessed at:
http://greengenes.secondgenome.com/downloads/phylochip_datasets

Supplementary References

1. **Jaffe DA, Prestbo E, Swartzendruber P, Weiss-Penzias P, Kato S, Takami A, Hatakeyama S, Kajii Y.** 2005. Export of atmospheric mercury from Asia. Atmos. Environ. **39**:3029-3038.
2. **Malm WC, Sisler JF, Huffman D, Eldred RA, Cahill TA.** 1994. Spatial and seasonal trends in particle concentration and optical extinction in the United States. J. Geophys. Res. **99(D1)**:1347–1370.
3. **Jaffe D, McKendry I, Anderson T, Price H.** 2003. Six "new" episodes of trans-Pacific transport of air pollutants. Atmos. Environ. **37**:391-404.

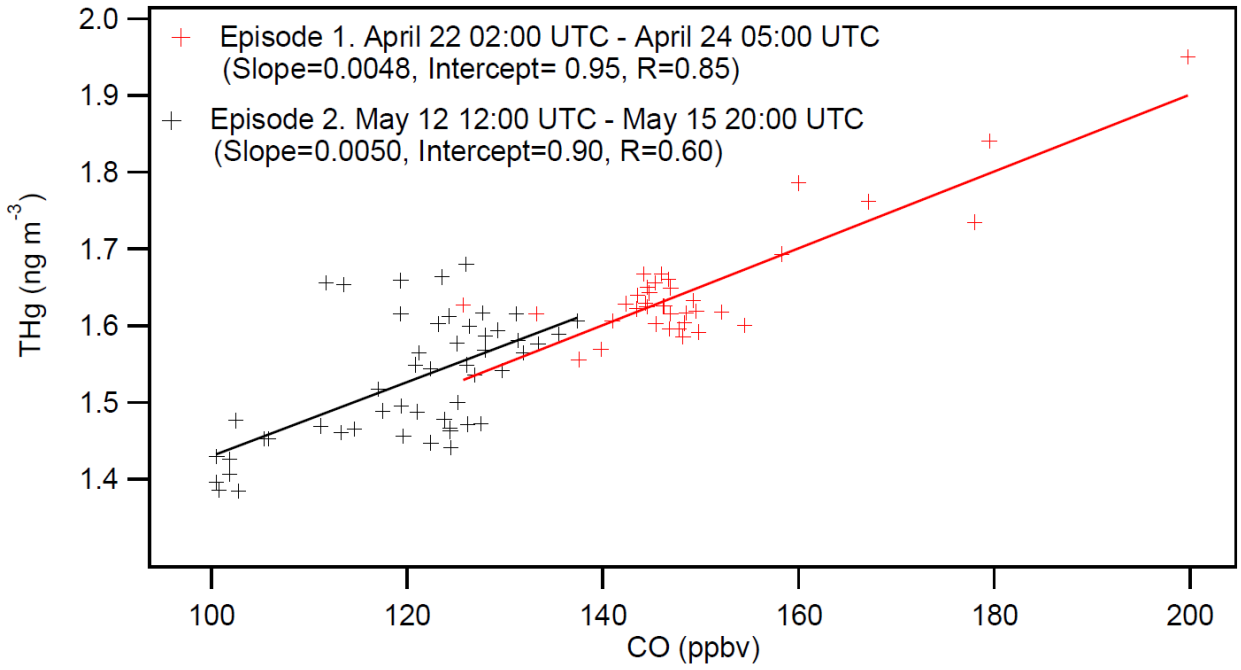

Figure S1. Total gaseous mercury (THg) and carbon monoxide (CO) data for 22-24 April (red) and 12-15 May (black) events. Enhancement ratios for both periods were indicative of Asian long-range transport based on analyses of similar pollution episodes measured at MBO (1).

a

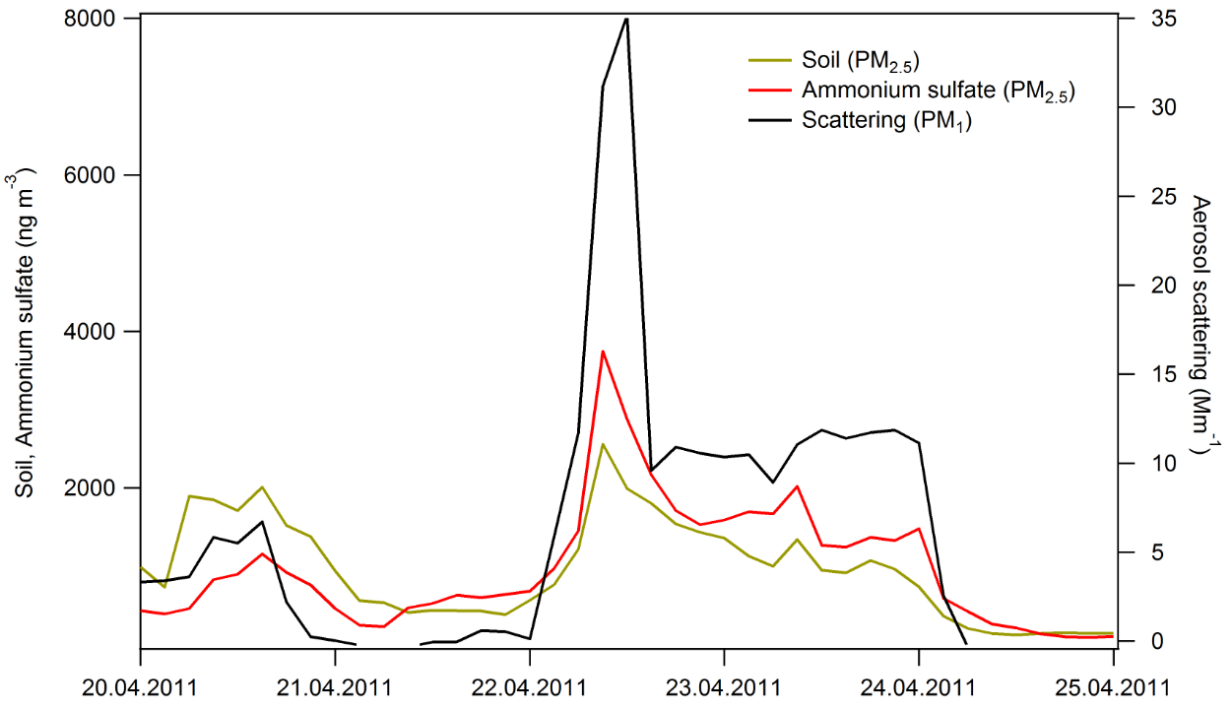

b

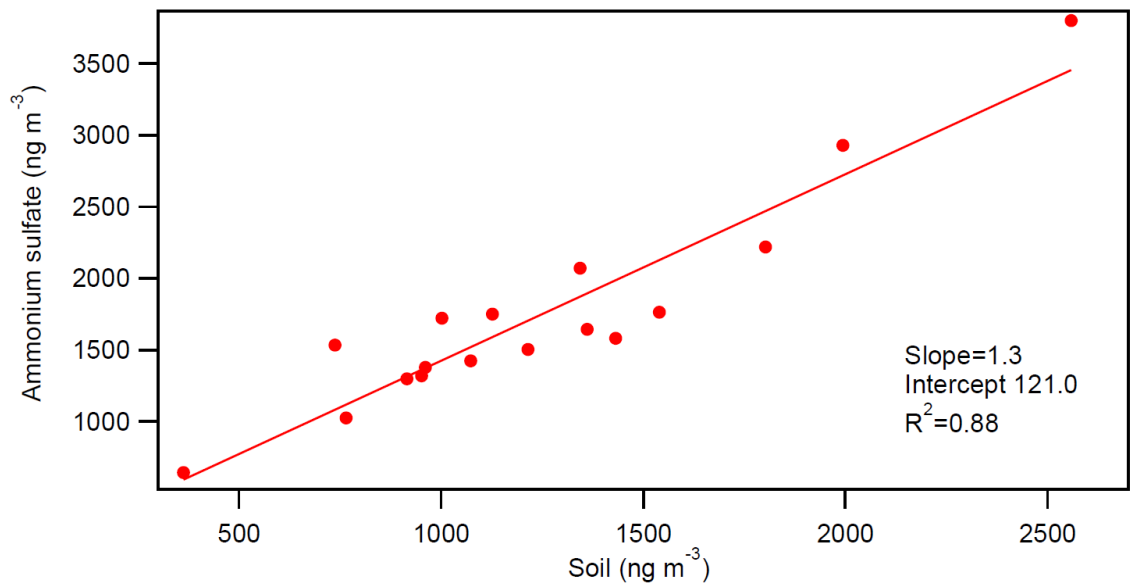

Figure S2. Soil (yellow), NH_4SO_4 (red), and aerosol (black) data for the April episode. Soil and NH_4SO_4 values were calculated using the Interagency Monitoring of Protected Visual Environments (IMPROVE) equations (2): [soil] = 2.2[Al] + 2.49[Si] + 1.63[Ca] + 2.42[Fe] + 1.94[Ti]; [NH_4SO_4] = 4.125*[S]. (**a**) Enhancements show the beginning, transition, and end of the event. (**b**) A high correlation coefficient between soil and NH_4SO_4 was observed (R^2 = 0.88), meaning the sampled air mass was aloft long enough for the species to mix (3).

a

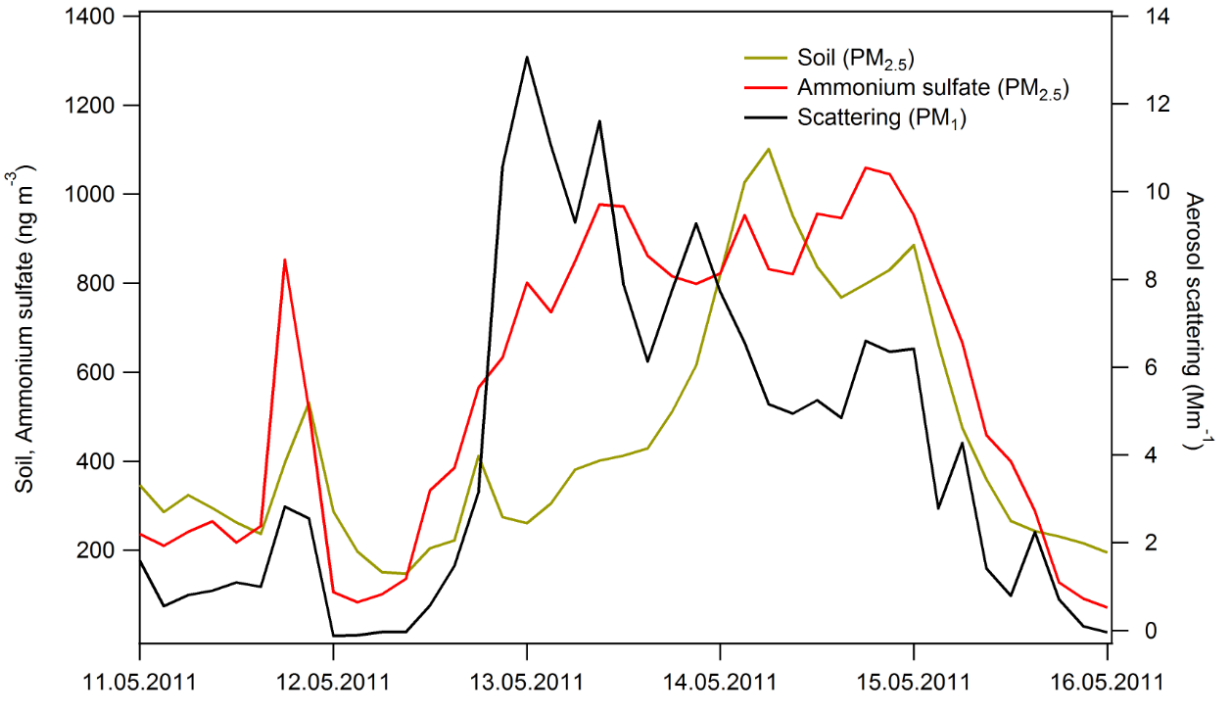

b

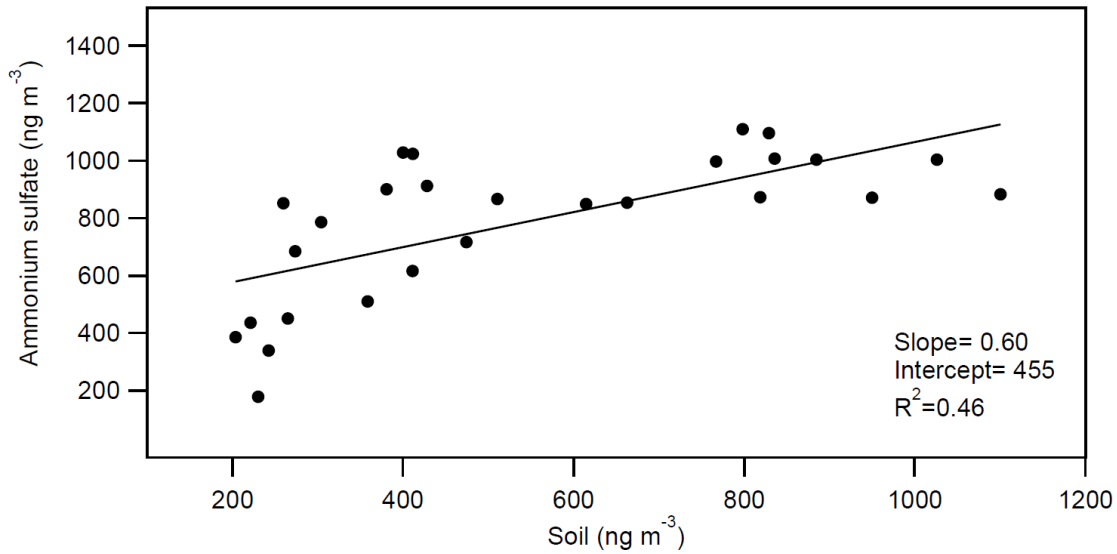

Figure S3. Soil (yellow), NH_4SO_4 (red), and aerosol (black) data for the May episode. Soil and NH_4SO_4 values were calculated using the Interagency Monitoring of Protected Visual Environments (IMPROVE) equations (2): [soil] = 2.2[Al] + 2.49[Si] + 1.63[Ca] + 2.42[Fe] + 1.94[Ti]; [NH_4SO_4] = 4.125*[S]. (**a**) Enhancements show the beginning, transition, and end of the event. (**b**) Compared to the April episode, a much lower correlation coefficient between soil and NH_4SO_4 (was observed (R^2 = 0.46), indicating substantial boundary layer influence during transpacific transport (3).

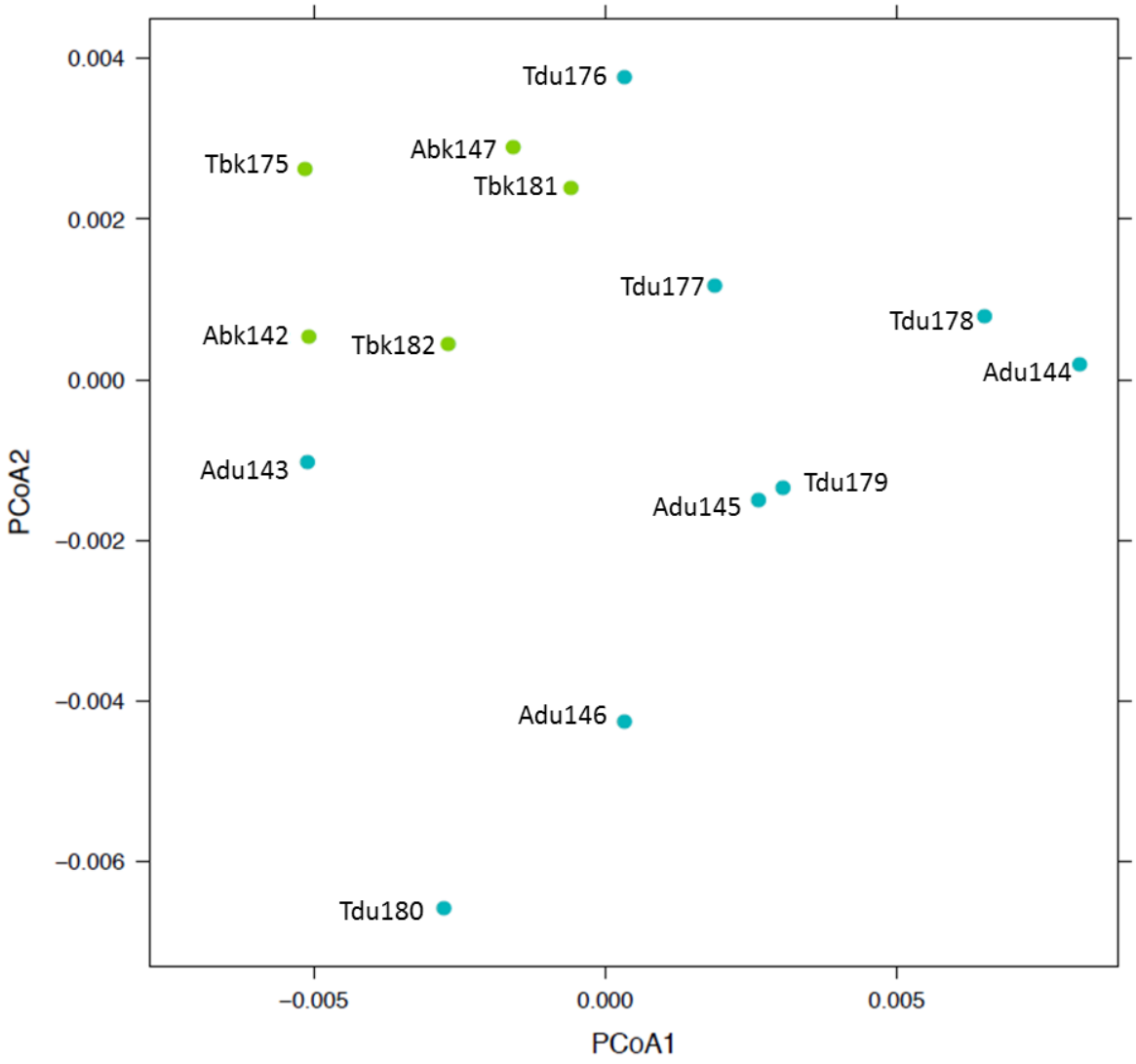

Figure S4. **Principle coordinate analysis of background samples (green) and plume samples (blue).** Analysis was based on weighted unifrac distance between samples from 2514 taxa with significant abundance differences. Axis 1: 50% of variation explained; Axis 2: 23% of variation explained. The partitioning shows the similarity in community composition between plume samples (-du-) and the similarity in community composition background samples (-bk-), regardless of plume timing (April or May). Note: Adu143 and Tdu176 were transitional samples at the onset of a plume (i.e., a mixture of background and plume).

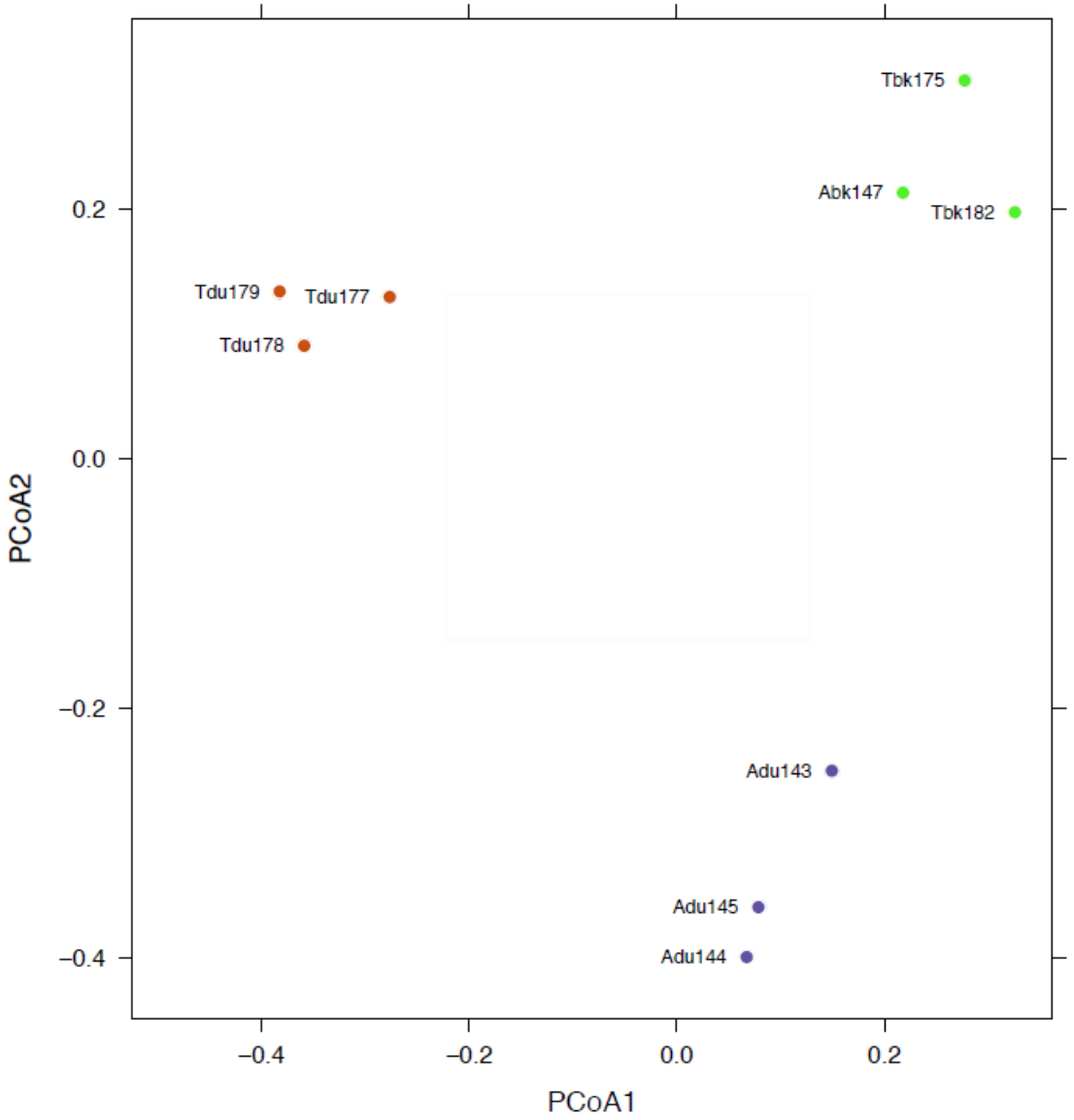

Figure S5. Principle coordinate analysis of April plume samples (purple), May plume samples (brown), and Background samples (green). Analysis was based on unweighted unifrac distance between samples from 86 selected taxa with incidence differences at peak plume intervals. Axis 1: 28% of variation explained; Axis 2: 26% of variation explained. The partitioning shows a microbiome contrast between the April and May plumes. Note: all samples were included in analysis but transitional points (i.e., a mixture of background and plume) were removed from the plot for clarity.

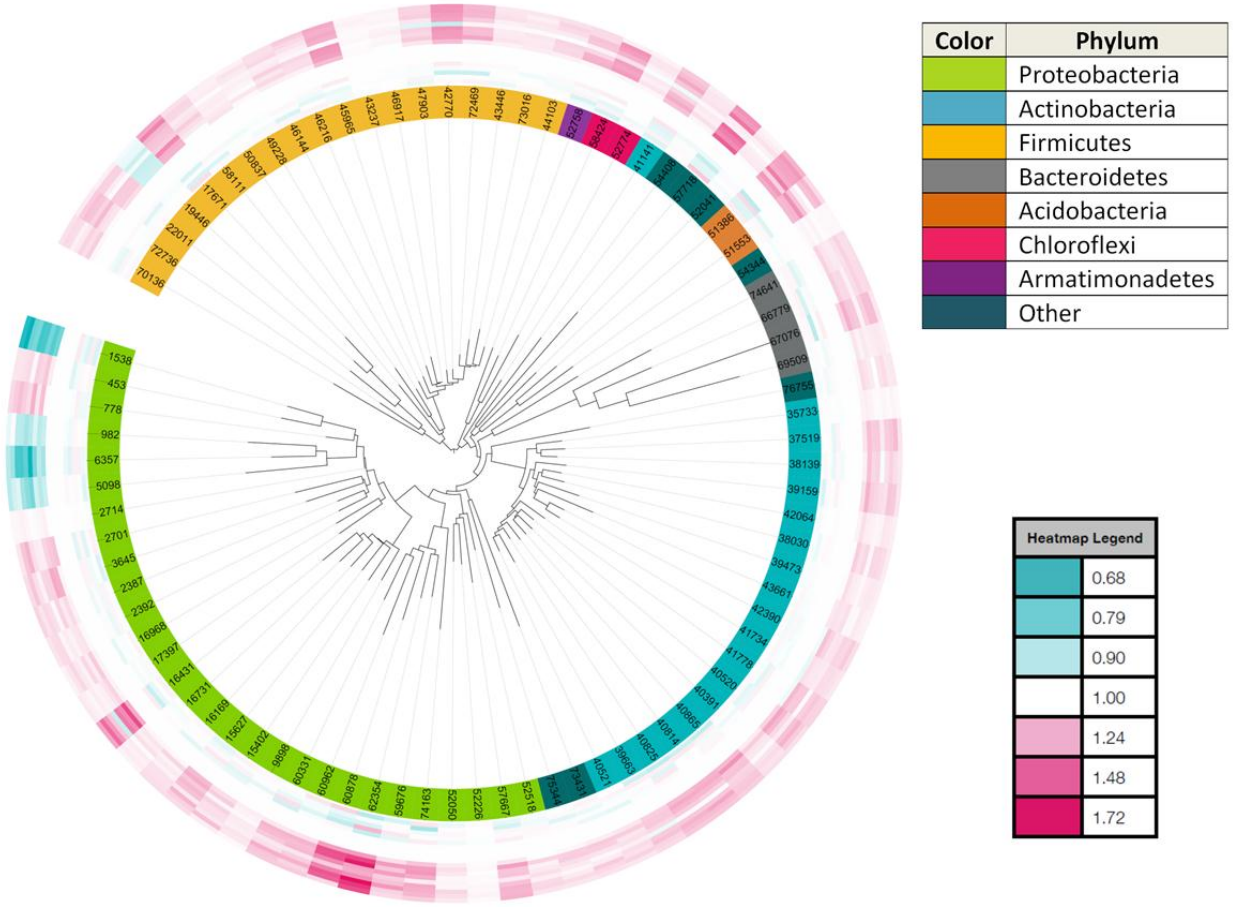

Figure S6. **Circular tree displaying taxonomic relationship of differentially abundant OTUs based on 16S rRNA gene alignment.** Families with significant abundance differences between background and plume samples from April and May events (Welch test *P* values < 0.001). Heat-map rings around the tree show increases or decreases in microbial abundance relative to combined category means: red indicates an increase in OTU abundance; blue indicates a decrease in abundance; and color saturation represents difference in intensity. Background samples are inner rings and plume samples are outer rings. Ring layer order follows the sample order in Tables 1 and 2 (e.g., the innermost outer ring is Adu143 and the outermost outer ring is Tdu180). Individual leaves on the tree, representing 83 families, have OTU identification numbers than can be used to locate more information at the microarray dataset archive (http://greengenes.secondgenome.com/downloads/phylochip_datasets).

Table S1. Archaea detected in April and May events

Sample	Class	Order	Family	Genus
Abk142	Methanomicrobia	Methanosarcinales	Unclassified	sfD
Adu144	Methanomicrobia	Methanosarcinales	Unclassified	sfD
Adu146	Methanomicrobia	Methanosarcinales	Unclassified	sfD
Tdu177	Methanomicrobia	Methanosarcinales	Unclassified	sfF
	pMC2A209	Unclassified	Unclassified	sfC
Tdu178	Methanomicrobia	Methanosarcinales	Unclassified	sfF
	Methanobacteria	Methanobacteriales	WSA2	unclassified
Tdu179	Methanomicrobia	Methanosarcinales	Unclassified	sfD
	Methanomicrobia	Methanosarcinales	Unclassified	sfF
Tdu180	Thermoprotei	Desulfurococcales	Desulfurococcaceae	Aeropyrum
Tbk182	Methanomicrobia	Methanosarcinales	Unclassified	sfF